HHS Public Access

Author manuscript

Circ Arrhythm Electrophysiol. Author manuscript; available in PMC 2019 February 01.

Published in final edited form as:

Circ Arrhythm Electrophysiol. 2018 February ; 11(2): e005852. doi:10.1161/CIRCEP.117.005852.

Altered Repolarization Reserve in Failing Rabbit Ventricular Myocytes: Calcium and Beta-adrenergic Effects on Delayed and Inward Rectifier Potassium Currents

Bence Hegyi, MD, PhD[1], **Julie Bossuyt, DVM, PhD**[1], **Kenneth S. Ginsburg, PhD**[1], **Lynette M. Mendoza, MBA, RDCS, FASE**[2], **Linda Talken**[3], **William T. Ferrier, DVM**[4], **Steven M. Pogwizd, MD, FAHA**[5], **Leighton T. Izu, PhD**[1], **Ye Chen-Izu, PhD, FAHA**[1,6,7], and **Donald M. Bers, PhD, FAHA**[1]

[1]Department of Pharmacology, University of California, Davis

[2]Echocardiography Laboratory, University of California, Davis Medical Center, Sacramento, CA

[3]School of Medicine, Dean's Office, University of California, Davis

[4]Surgical Research Facility, School of Medicine, University of California, Davis

[5]Department of Medicine, University of Alabama at Birmingham, Birmingham, AL

[6]Department of Biomedical Engineering, University of California, Davis

[7]Department of Internal Medicine/Cardiology, University of California, Davis

Abstract

Background—Electrophysiological remodeling and increased susceptibility for cardiac arrhythmias are hallmarks of heart failure (HF). Ventricular action potential (AP) duration (APD) is typically prolonged in HF, with reduced repolarization reserve. However, underlying K^+ current changes are often measured in non-physiological conditions (voltage-clamp, low pacing rates, cytosolic Ca^{2+} buffers).

Methods and Results—We measured the major K^+ currents (I_{Kr}, I_{Ks}, I_{K1}) and their Ca^{2+}- and beta-adrenergic dependence in rabbit ventricular myocytes in chronic pressure/volume overload-induced HF (vs. age-matched controls). APD was significantly prolonged only at lower pacing rates (0.2–1 Hz) in HF under physiological ionic conditions and temperature. However, when cytosolic Ca^{2+} was buffered, APD prolongation in HF was also significant at higher pacing rates. Beat-to-beat variability of APD was also significantly increased in HF. Both I_{Kr} and I_{Ks} were significantly upregulated in HF under AP-clamp, but only when cytosolic Ca^{2+} was not buffered. CaMKII inhibition abolished I_{Ks} upregulation in HF, but it did not affect I_{Kr}. I_{Ks} response to beta-adrenergic stimulation was also significantly diminished in HF. I_{K1} was also decreased in HF regardless of Ca^{2+} buffering, CaMKII inhibition or beta-adrenergic stimulation.

Correspondence: Donald M. Bers, PhD, Department of Pharmacology, University of California, Davis, 451 Health Sciences Drive, Davis, CA 95616, Tel: (530) 752-6517, Fax: (530) 752-7710, dmbers@ucdavis.edu.

Disclosures: None.

Conclusions—At baseline Ca^{2+}-dependent upregulation of I_{Kr} and I_{Ks} in HF counterbalances the reduced I_{K1}, maintaining repolarization reserve (especially at higher heart rates) in physiological conditions, unlike conditions of strong cytosolic Ca^{2+} buffering. However, under beta-adrenergic stimulation, reduced I_{Ks} responsiveness severely limits integrated repolarizing K^+ current and repolarization reserve in HF. This would increase arrhythmia propensity in HF, especially during adrenergic stress.

Journal Subject Terms

Electrophysiology; Ion Channels/Membrane Transport; Heart failure

Keywords

Heart failure; electrophysiology; potassium channels; action potential; calcium/calmodulin-dependent protein kinase II; delayed rectifier potassium current; inward rectifier potassium current; beta-adrenergic stimulation

INTRODUCTION

Heart failure (HF) is known to induce profound electric remodeling affecting the repolarization process of the cardiac action potential (AP) resulting in increased risk for cardiac arrhythmias. HF patients with prolonged heart rate-corrected QT interval (QT_c) in their electrocardiogram are thought to have higher risk for electric abnormalities and sudden cardiac death;[1–3] although details are debated,[4, 5] and more than half of HF patients exhibit normal QT_c.[2–6] Meanwhile, in isolated ventricular myocytes AP duration (APD) is typically reported to be prolonged both in human HF[7, 8] and animal HF models.[9–12] However, in those studies APD prolongation was most pronounced at low pacing rates and when cytosolic Ca^{2+} was buffered (i.e. non-physiological conditions). Moreover, no APD prolongation was found above 1 Hz pacing frequency in human,[8] canine,[13] and rabbit[14] failing myocytes, in line with observations that differences in QT intervals between healthy controls and HF patients was abolished at high heart rates.[15]

Earlier studies demonstrated that reduced K^+ currents, enhanced Na^+/Ca^{2+} exchange and increased late Na^+ currents contribute to APD prolongation in HF.[7–14, 16] But these data were obtained in non-physiological conditions (rectangular voltage clamp pulses vs. AP clamp, long cycle lengths and with cytosolic Ca^{2+} transients eliminated by Ca^{2+} buffers). In addition to direct Ca^{2+}effects on channel gating, Ca^{2+}/calmodulin-dependent protein kinase II (CaMKII) activation requires locally high $[Ca^{2+}]_i$ levels. Importantly, CaMKII is also known to be upregulated and more active in HF[17] and has been shown to modulate Na^+ and K^+ channel gating and can also alter channel expression levels[18, 19] that shape the cardiac AP and contribute to arrhythmogenesis in HF.[20, 21] This regulatory action of CaMKII on ionic currents might have been underestimated in previous HF studies using non-physiological conditions for recordings.

In this study, we aimed to measure the actual repolarizing K^+ currents that occur under physiological AP-clamp recording conditions to assess the modulatory effect of CaMKII by $[Ca^{2+}]_i$ transients and β-adrenergic receptor (β-AR) activation. We hypothesized that

increased $[Ca^{2+}]_i$ and CaMKII activity under physiological conditions play a role in the attenuated AP prolongation at higher pacing rates in HF vs. control. Specifically, we measured APs and three major repolarizing K^+ currents during phase 3 of the AP: the rapid and slow components of delayed rectifier K^+ currents (I_{Kr} and I_{Ks}, respectively) and the inward rectifier K^+ current (I_{K1}) in HF and age-matched control rabbit ventricular myocytes. We used a previously well-characterized chronic non-ischemic HF rabbit model (combined volume and pressure overload), which is also arrhythmogenic.[11, 17, 21–25] We used the AP-clamp technique at 2 Hz pacing both with preserved $[Ca^{2+}]_i$ transients[26, 27] and with $[Ca^{2+}]_i$ buffered below the diastolic level. Modulation of these K^+ currents by Ca^{2+}, CaMKII and β-AR stimulation was also examined to assess the changes of the repolarization reserve in pathophysiological settings characteristic of HF.[11, 20]

METHODS

The data, analytic methods, and study materials will not be made available to other researchers for purposes of reproducing the results or replicating the procedure.

All animal handling and laboratory procedures were in accordance with the approved protocols of the local Institutional Animal Care and Use Committee confirming to the *Guide for the Care and Use of Laboratory Animals* published by the US National Institute of Health (8th edition, 2011).

Arrhythmogenic rabbit non-ischemic HF model

HF was induced in New Zealand White rabbits (all male, 2.5–3 kg, 3–4-month-old) by combined aortic insufficiency and afterwards abdominal aortic stenosis as previously described.[22] HF progression was monitored by echocardiography and myocytes were isolated when left ventricular end-systolic dimension exceeded 1.55 cm (Table 1). Similar to our previous studies in this rabbit model, the hearts used here were increased in weight by ~100%, dilated (LVEDD) and exhibited reduced fractional shortening (FS). HF animals also exhibited abdominal ascites fluid and evidence of lung edema (LW and LW/BW).

For myocyte isolation, rabbits were subjected to general anesthesia (induction with propofol 2 mg/kg followed by 2–5% isoflurane in 100% oxygen). After thoracotomy, the heart was quickly excised and rinsed in cold nominally Ca^{2+}-free MEM. The right atrium was removed and the aorta opened to visualize the left coronary ostium which was then cannulated using a 5F Judkins right catheter (Performa; Merit Medical Systems). Perfusion of the LV and LA was established before removal of the RV free wall and application of a purse-string suture to secure the catheter in place. The remainder of the isolation procedure was then essentially as previously described.[28] Cells isolated from healthy age-matched rabbits were used for control experiments.

Electrophysiology

Isolated cells were transferred to a temperature controlled plexiglass chamber (Cell Microsystems) and continuously superfused with a bicarbonate containing Tyrode solution with the following composition (in mmol/L): NaCl 124, $NaHCO_3$ 25, KCl 4, $CaCl_2$ 1.2, $MgCl_2$ 1, HEPES 10, Glucose 10, with pH = 7.4. APs and underlying ion currents were

recorded in whole-cell configuration of patch-clamp technique. Electrodes were fabricated from borosilicate glass (World Precision Instruments) with tip resistances of 2–2.5 MΩ when filled with internal solution containing (in mmol/L): K-Aspartate 110, KCl 25, NaCl 5, Mg-ATP 3, HEPES 10, cAMP 0.002, phosphocreatine-K_2 10, and EGTA 0.01, with pH = 7.2. This composition preserved the physiological $[Ca^{2+}]_i$ transient and contraction of the myocytes.[29] To study the Ca^{2+}-dependence of ionic currents in HF, $[Ca^{2+}]_i$ was buffered to nominally zero by adding 10 mM BAPTA to the above listed pipette solution. The electrodes were connected to the input of an Axopatch 200B amplifier (Axon Instruments). Outputs from the amplifier were digitized at 50 kHz using Digidata1440A A/D card (Molecular Devices) under software control (pClamp 10). The series resistance was typically 3–5 MΩ and it was compensated by 85%. Experiments were discarded when the series resistance was high or increased by more than 10% during the experiment. Reported AP voltages are already corrected to the liquid junction potentials. All experiments were conducted at 37±0.1°C.

APs were recorded in current-clamp experiments where cells were stimulated with supra-threshold depolarizing pulses (2 ms duration) delivered via the patch pipette at various pacing frequencies between 0.2 Hz and 5 Hz. After reaching steady-state at each frequency (3 min pacing at a given frequency), 50 consecutive APs were recorded to examine the average behaviour. APD at 95% of repolarization (APD_{95}) was used to assess precisely the influence of NCX function – which is known to be altered in HF[22] - on AP profile when measured under physiological conditions.[29] Series of 50 consecutive APs were analysed to estimate short-term variability (STV) of AP duration according to the following formula: $STV = \Sigma (\left| APD_{i+1} - APD_i \right|)/[(n_{beats} -1) \times \sqrt{2}]$, where APD_n and APD_{n+1} indicate the durations of the i^{th} and $(i+1)^{th}$ APs, and n_{beats} denotes the number of consecutive beats analysed.[30, 31] Changes in STV are presented as Poincaré plots, where 50 consecutive APD_{95} values are plotted, each against the duration of the previous AP.

AP-clamp Sequential Dissection experiments were conducted as previously described.[26] All currents were recorded after their specific blocker had reached steady-state effect (~2 min perfusion). The following sequence of blockers was used to measure the major K^+ currents: 1 μM HMR-1556 for I_{Ks}, 1 μM E-4031 for I_{Kr}, 100 μM $BaCl_2$ for I_{K1}. Experiments were performed both when Ca^{2+} cycling was preserved (Physiol) and when $[Ca^{2+}]_i$ was buffered below the diastolic level using 10 mM BAPTA in the pipette solution ($BAPTA_i$) to compare the Ca^{2+}-sensitivity of these K^+ currents during AP. To test the effect of CaMKII, cells were pretreated for ~2 hours with the specific CaMKII inhibitor, autocamtide-2-related inhibitory peptide (AIP, cell-permeable myristoylated form, 1 μM) before starting the experiment, and both the perfusion and pipettes solutions were also supplemented with AIP. In experiments examining the effect of β-AR stimulation on K^+ currents, isoproterenol (ISO, 3–300 nM) was applied on AP-clamped cells. When ISO reached a steady-state effect (~2 min), then the K^+ current blockers were added to the perfusion solution in a cumulative manner to measure I_{Ks}, I_{Kr} and I_{K1}. Experiments were excluded from analysis if significant rundown of L-type Ca^{2+} current was observed (in periodic tests) or the membrane current following ISO stimulation did not reach steady-state.

Ion currents were normalized to cell capacitance, determined in each cell using short (10 ms) hyperpolarizing pulses from −10 mV to −20 mV. Cell capacitance was 191.68±3.60 pF in HF (n=116 cells/10 animals) vs. 144.52±1.45 pF in age-matched controls (75 cells/5 animals) using two sample Student's *t* test, $p<0.001$.

Chemicals and reagents were purchased from Sigma-Aldrich, if not specified otherwise. E-4031 and HMR-1556 were from Tocris Bioscience.

Statistical analysis

Data are expressed as Mean±SEM. The number of cells in each experimental group was reported in the figures and/or figure captions as *n* = number of cells/number of animals. Cells in each group came from at least three individual animals. Statistical significance of differences was evaluated using one-way or two-way ANOVA to compare multiple groups and a Bonferroni posttest was used for pairwise comparisons. Differences were deemed significant if $p<0.05$.

RESULTS

Frequency- and Ca2+-dependent changes of AP in HF

Figure 1 shows representative APs and group analysis in HF and age-matched Control (abbreviated as Ctl in Figs) myocytes, and first we consider the physiological case with normal Ca^{2+} cycling (Physiol; Fig. 1A–B). APD_{95} was significantly longer in HF vs. Control at 1 Hz pacing (271.8±15.2 ms vs. 197.8±6.9 ms, respectively, $p<0.001$) (Fig. 1C). As pacing rate was reduced, APD_{95} progressively increased in HF, but not in Control, making the Control-HF difference larger (Fig. 1C). The anomalous APD shortening in rabbit ventricle at very low pacing rates has been attributed to slowly-recovering transient outward K^+ current ($I_{to,s}$) that is normally suppressed at physiological heart rates.[32] Notably, at higher physiological stimulation rates (2–5 Hz) APD_{95} was not significantly different in HF vs. Control (218.9±13. ms vs. 204.2±7.7 ms at 2 Hz in HF and Control, respectively).

Buffering $[Ca^{2+}]_i$ to very low levels with 10 mM BAPTA in the pipette ($BAPTA_i$) also prevented $[Ca^{2+}]_i$ transients, and resulted in longer APD in general compared to the physiological solution (Fig. 1C, E-F). Moreover, with $BAPTA_i$ significant APD prolongation was observed in HF vs. Control at all pacing frequencies studied (Fig. 1C), although the absolute difference became smaller with increasing frequency.

AP plateau height, characterized as mid-plateau potential ($V_{mid\text{-}plateau}$) was less positive in HF at all frequencies studied for the $BAPTA_i$ case, and for the physiological case as well (except for 0.2–1 Hz; Fig. 1D). The extent of plateau depression at 2–5 Hz was greater with buffered $[Ca^{2+}]_i$ than for physiological pipette solution (HF-Physiol vs. HF-$BAPTA_i$, Fig. 1D). Consistent with this, early repolarization rate and magnitude (AP phase 1) were both reduced in HF under both pipette conditions (Fig. 1A–B, 1E-F). Resting membrane potential (V_{rest}) was slightly more positive in HF and AP peak voltage (V_{peak}) was significantly lower in HF under both conditions (Fig. 1G). In line with this, the AP maximum rate of rise (dV/dt_{max}) was also decreased by ~25% in HF (Fig. 1H), which might reflect the altered Na^+ channel availability at more positive V_{rest}, but contributions of decreased Na^+ channel

functional expression or elevated $[Na^+]_i$ cannot be ruled out. Importantly here, the maximum rate of repolarization ($-dV/dt_{max}$) during AP phase 3 was also significantly decreased in HF vs. Control myocytes under physiological conditions and more markedly so with $BAPTA_i$ (Fig. 1H).

HF rabbit myocytes also exhibited increased temporal variability of APD_{95} compared to myocytes from Control hearts (Ctl; Fig. 2A). The short-term variability (STV) calculated using 50 consecutive APD_{95} values was significantly increased at 1 Hz pacing in HF vs. Control (HF-Physiol vs. Ctl-Physiol, 4.65±0.43 ms vs. 3.04±0.23 ms, respectively, $p<0.01$), and at 2 Hz as well, where mean APD_{95} did not differ in HF vs. Control (Fig. 2B). However, these differences became smaller at higher frequencies. We also analyzed the cumulative distribution of beat-to-beat changes in APD_{95}. More than half of consecutive beats have less than 5 ms difference (both Control and HF), but for HF a larger percentage of beats exhibited more than 5 and 10 ms difference from beat to beat, apparent as “long-tails” in the cumulative distribution curves (Fig. 2C–D). This difference was less with $BAPTA_i$.

Spontaneous SR Ca^{2+} release (or leak) and consequent afterdepolarizations are known to contribute to increased beat-to-beat variability of APD,[30] and are known to occur more frequently in this HF model at a given SR Ca^{2+} load (CaMKII-dependently).[17, 33, 34] However, at baseline in steady-state pacing neither early nor delayed afterdepolarizations (EAD, DAD) were observed in either Control or HF. Therefore, to test the SR Ca^{2+} store stability we paced the cells at 2 Hz for 5 min, then paused to record V_m without stimulation. DADs developed in 10/12 HF cells and among them 5 cells also exhibited spontaneous APs likely to be triggered by SR Ca release (Fig. 2E shows an example). Average DAD frequency was 1.14±0.31/min, with average amplitude of 3.15±0.19 mV. Only 15% of DADs were larger than 5 mV in amplitude (not including those that triggered APs). However, neither the age-matched controls cells (0/12 cells) nor HF cells pretreated with CaMKII inhibitory peptide AIP (1 μM) (0/10 cells) showed such arrhythmogenic activities (Fig. 2E). Thus, higher SR Ca^{2+} instability may contribute to the higher beat-to-beat APD variability in HF (Fig. 2C–D), that was suppressed by $BAPTA_i$.

Changes in magnitude and dynamics of I_{Kr}, I_{Ks} and I_{K1} under AP in HF

The APD data suggest complex remodeling in HF and the involvement of Ca^{2+}-dependent processes in the altered repolarization phase at higher physiological rabbit pacing rates. Thus, we studied the major repolarizing K^+ currents (I_{Kr}, I_{Ks}, I_{K1}) during phase 3 of the AP at 2 Hz. All three ionic currents were recorded from the same myocyte, employing the AP-clamp Sequential Dissection technique[26] with preserved $[Ca^{2+}]_i$ cycling condition (Physiol) and also with $[Ca^{2+}]_i$ buffered with 10 mM BAPTA in the pipette ($BAPTA_i$). Involvement of CaMKII pathway was also investigated in the Ca^{2+}-dependent alteration of repolarization. A previously recorded typical rabbit ventricular AP was used as voltage command in all AP-clamp experiments (canonical AP-clamp) at 2 Hz. This typical AP has an APD_{95} of 205.5 ms, which is not significantly different from the APD_{95} of either Control or HF cells at 2 Hz (one sample *t* test). Because significant cellular hypertrophy was found in HF (~33% increase in cell capacitance, see Methods for details) all reported currents are normalized to the corresponding cell capacitance.

The rapid component of delayed rectifier potassium current (I_{Kr}) was measured as E-4031-sensitive current under AP-clamp (Fig. 3A–C). Peak I_{Kr} density was 18% higher in HF myocytes compared to age-matched controls when measured in our physiological condition (1.13±0.02 vs. 0.96±0.02 A/F in HF and Control, respectively, $p<0.001$; Fig. 3A,D). In contrast, with $BAPTA_i$ peak I_{Kr} density was 7% smaller in HF vs. Control (0.86±0.02 vs. 0.92±0.02 A/F, respectively, $p<0.05$; Fig. 3B,D). AIP pretreatment to inhibit CaMKII affected neither peak I_{Kr} density nor integrated charge carried by I_{Kr}, in either Control or HF (Fig. 3C,D,F), suggesting that CaMKII is not involved in acute I_{Kr} modulation. On the other hand, I_{Kr} is elevated earlier during the AP in HF vs. Control (Fig. 3E), regardless of $[Ca^{2+}]_i$ (Fig. 3A vs. B and 3E), indicating altered I_{Kr} gating in HF. The slight increase in peak and integrated I_{Kr} under physiological conditions here, could easily be missed if I_{Kr} is measured under non-physiological conditions (e.g. $BAPTA_i$).

The slow component of delayed rectifier K^+ current (I_{Ks}) was measured as HMR-1556-sensitive current under AP-clamp (Fig. 4A–C). I_{Ks} is a tiny current in the absence of β-AR stimulation in healthy ventricular myocytes (Fig. 4A), consistent with minimal effects of I_{Ks} block on baseline APD in rabbit ventricle.[35] Surprisingly, we found a 42% increase in basal I_{Ks} magnitude in HF vs. Control in our physiological condition (0.34±0.03 vs. 0.24±0.02 A/F, respectively, $p<0.01$; Fig. 4A,D-F). Furthermore, the increase in I_{Ks} was not observed with $BAPTA_i$ (Fig. 4B) or when HF cells were pretreated with AIP (Fig. 4C–F). We infer that Ca^{2+}-dependent CaMKII activity may acutely increase I_{Ks} in HF.

The inward rectifier K^+ current (I_{K1}) was measured as Ba^{2+}-sensitive current (Fig. 5A–C). Peak I_{K1} density during repolarization was 25% smaller in HF vs. Control (2.28±0.11 vs. 3.04±0.12 A/F, respectively, $p<0.001$; Fig. 5A, D). Mid-plateau and integrated I_{K1} over the APD was also smaller in HF vs. Control (Fig. 5E–F). Neither buffering $[Ca^{2+}]_i$ ($BAPTA_i$) nor CaMKII inhibition (AIP) altered this conclusion (Fig. 5B,C). We conclude that I_{K1} downregulation in this HF model is not mainly due to acute effects of $[Ca^{2+}]_i$ or CaMKII on I_{K1}, but might reflect lower functional expression level of the channel proteins. Since CaMKII is upregulated in HF[17] and can cause reduced functional expression of $K_{ir}2.1$ and I_{K1},[19] this does not preclude an indirect chronic effect of CaMKII on I_{K1} functional expression in HF.

Altered β-adrenergic response of K^+ currents in HF

Increased sympathetic activation and altered β-AR responses are frequently reported in HF. Therefore, we also tested effects of β-AR stimulation on I_{Kr}, I_{Ks} and I_{K1} in HF and Control myocytes using AP-clamp. Because both protein kinase A (PKA) and CaMKII are known to mediate downstream effects of β-AR stimulation and the activity of these kinases are also known to be altered in HF, we again measured ionic currents with physiological preserved $[Ca^{2+}]_i$ cycling and with heavily buffered $[Ca^{2+}]_i$.

I_{Ks} increased robustly upon treatment with the non-specific β-AR agonist isoproterenol (ISO, 10 nM; Fig. 6A,D). Buffering $[Ca^{2+}]_i$ limited I_{Ks} response, indicating the involvement of Ca^{2+} and/or CaMKII (as well as PKA) in mediating ISO effect on I_{Ks}. However, the ISO-induced increase in I_{Ks} peak density was much reduced in HF both with $[Ca^{2+}]_i$ cycling (7.25-fold in Control vs. 2.91-fold increase in HF) and with $BAPTA_i$ (3.85-fold in Control

vs. 2.88-fold in HF; Fig. 6D). The ISO-induced increase in I_{Ks} in the presence of Ca^{2+} was not simply a scaled-up version of the $BAPTA_i$ traces, but a more prominent increase during the plateau, resulting in an even greater increment in integrated charge carried by I_{Ks} (Fig. 6A,D). Even after ISO, the integrated K^+ efflux during the AP in HF was less than half of that in Control (Fig. 6D), which could seriously limit repolarization reserve.

I_{Kr} was affected minimally upon ISO-stimulation (Fig. 6B,E), which achieved statistical significance only in Control cells and physiological solutions (8.1% increase in I_{Kr} peak density and 23.1% increase in total charge carried during the AP, $p<0.05$ in both cases). As in Fig. 3, I_{Kr} was higher at baseline in HF vs. Control, but failed to increase significantly upon ISO exposure (Fig. 6E).

I_{K1} peak density was not affected by beta-adrenergic stimulation. (Fig. 6C,F). However, the I_{K1} net charge increased significantly (by 23%) following ISO application in Control, but not in HF cells, when measured with cycling $[Ca^{2+}]_i$ under AP-clamp (Fig. 6F), possibly reflecting some Ca^{2+}-dependent rectification of I_{K1} as previously described.[27, 36]

Because the ISO effect on I_{Ks} was blunted in HF vs. Control, we tested whether the β-AR effects were due to decreased ISO-sensitivity or limited maximal response. We varied ISO between 3 and 300 nM in AP-clamped HF and Control cells (Fig. 7). Since steady-state contracting AP-clamped myocytes were unstable at the higher ISO concentrations without $[Ca^{2+}]_i$ buffering, these experiments were performed with 10 mM BAPTA in the pipette. ISO dose-dependently increased I_{Ks} both in Control and HF cells with nearly identical EC_{50} values (8.39±0.85 nM and 8.90±1.61 nM, respectively, n.s.) and Hill coefficients (Fig. 7A). However, the maximum response was only half as much in HF vs. Control (4.0-fold vs. 8.4-fold increase in peak I_{Ks} density, respectively) indicating unchanged ISO-sensitivity, but significant hyporesponsiveness of I_{Ks} to ISO. I_{Kr} increased only following ISO application and no difference was seen between Control and HF regarding EC_{50} values and maximal responses (Fig. 7B). Finally, peak I_{K1} density during the AP did not show any change, even at high concentration of ISO, but I_{K1} was again significantly reduced in HF (Fig. 7C).

Relative contributions of each K^+ current to AP phase 3 repolarization

AP repolarization is governed by the dynamic time-and voltage-dependent activation of K^+ currents. Each K^+ current has its unique fingerprint (current shape under the changing voltages of AP) and different magnitude during the cardiac AP. The relative contributions of the major K^+ currents (I_{Kr}, I_{Ks} and I_{K1}) involved in the phase 3 repolarization of AP in control and in HF are shown in Fig. 8 analyzed at different points of repolarization (+20, −20 and −60 mV) and as integrated K^+ flux during the AP (Fig. 8, insets).

First, we consider physiological solutions with Ca^{2+} cycling at baseline (Fig. 8A–B) where total repolarizing K^+ current is unaltered in HF vs. Control at either −20 mV, −60 mV or the integral. However, the reduced I_{K1} in HF is largely compensated by increases in both I_{Kr} and I_{Ks}, and this balance may allow the relatively maintained APD_{95} observed in HF myocytes at 2–5 Hz stimulation (Fig. 1B–C). In Control myocytes ISO greatly increases I_{Ks} and reverses the I_{Kr} vs. I_{Ks} dominant pattern of AP repolarization. However, in HF myocytes hyporesponsive of I_{Ks} to β-AR stimulation, I_{Ks} remains less than I_{Kr}, such that the combined

I_{Ks}+I_{Kr} do not compensate for the reduced I_{K1} and integrated K^+ current is substantially reduced in HF (Fig. 8C).

CaMKII inhibition with AIP affected only I_{Ks}, but because basal I_{Ks} is a tiny current under physiological AP, it does not significantly alter the magnitude of the net K^+ current (Fig. 8D). Buffering cytosolic Ca^{2+} below diastolic level abolishes the upregulation of both I_{Kr} and I_{Ks} in HF, resulting in a pronounced decrease in net K^+ current (Fig. 8E). Isoproterenol in the presence of $BAPTA_i$ exacerbated the difference between HF and Control because under those conditions I_{K1}, I_{Ks} and I_{Kr} are all reduced in HF compared to Control (Fig. 8F).

DISCUSSION

Action potential duration changes in HF

There is consensus that HF is associated with lengthening of the ventricular APD (and corrected QT intervals, QT_c). This is supported by evidence from numerous experimental studies involving several species and multiple methods to induce HF.[7–14] However, HF-associated APD differences in previous studies often used lower pacing rates. In humans HF was associated with a 50 ms difference in baseline QT_c, but as heart rate increased during exercise, the QT_c values converged and were not different between Control and HF.[15] In agreement with these observations, we found longer APD in HF vs. Control in rabbits at 0.2–1 Hz pacing, but not at higher physiological pacing rates for rabbits (Fig. 1). However, when the $[Ca^{2+}]_i$ was buffered, APD was prolonged in HF at all stimulation rates, suggesting a role for Ca^{2+}-dependent processes in shaping the AP morphology in HF.

Patients with QT_c prolongation have increased risk for sudden cardiac death almost independent of the etiology of disease.[37] Substantial QT_c prolongation, especially in end-stage HF and in ischemic origin, indicates higher risk for cardiac arrhythmias also in HF.[4] However, data also suggest that short-term QT_c-variability may be a better predictor of sudden cardiac death than QT_c interval per se.[5, 38] In our arrhythmogenic HF model, STV of APD_{95} was also significantly increased (Fig. 2). It was reported that STV depends critically on the baseline APD_{95}.[31] In our case, STV was increased in HF vs. Control at 2 Hz pacing, despite no difference in baseline APD_{95}. Interestingly, in our HF data a higher fraction of APs showed large difference in APD_{95} in subsequent beats (Fig. 2C–D) despite unaltered mean APD_{95}. Because strong $[Ca^{2+}]_i$ buffering suppressed this effect, it seems likely due to Ca^{2+}-related events (e.g. SR Ca^{2+} releases) rather than remodeling in ionic currents and their different contribution to STV.[31] Accordingly, spontaneous SR Ca^{2+} leak, Ca^{2+} sparks and waves can contribute to increased beat-to-beat variability.[30] Even without overt EAD or DAD induction during steady-state pacing, local Ca^{2+} events could readily cause APD variations. Indeed, we saw such events following trains of stimuli in HF that were prevented by CaMKII inhibition, and were not seen in Control cells. This is consistent with higher SR Ca^{2+} leak and Ca^{2+} waves measured in this arrhythmogenic rabbit HF model (at matched SR Ca^{2+} load) which was also sensitive to CaMKII inhibition.[17, 24, 33, 34, 39] This higher SR Ca^{2+} leak associated with HF may contribute to increased beat-to-beat variability of APD, however, further studies are needed to define the precise relationship between these two important parameters of HF.

Changes in repolarizing K^+ currents in HF that shape the AP

In this study, we systematic characterize the major K^+ currents (I_{Kr}, I_{Ks}, I_{K1}) underlying phase 3 AP repolarization in Control and HF myocytes, including Ca^{2+}- and β-AR-dependent properties. Decreased transient outward K^+ current (I_{to}) in HF has been reported in several models, including ours.[7, 11, 40] Consistent with that, we saw reduced phase 1 AP repolarization in HF (Fig. 1). However, our focus here is on the K^+ currents that dominate phase 3 repolarization.

To understand how I_{Kr}, I_{Ks} and I_{K1} are altered in shaping the APD in HF, we used our sequential dissection method that allows all three K^+ currents to be measured in the same myocyte under relatively physiological AP conditions. Often these individual currents are measured independently, with square voltage clamp pulses and under relatively non-physiologic conditions, including prevention of $[Ca^{2+}]_i$ transients. Since Ca^{2+}-dependent properties can influence several K^+ currents, and to compare with prior work, we did parallel measurements with strong $[Ca^{2+}]_i$ buffering.

In previous studies, most K^+ currents were found to be downregulated in HF. In our study, I_{K1} density was indeed lower in HF under all conditions, regardless of $[Ca^{2+}]_i$ buffering, CaMKII inhibition or β-AR activation in agreement with prior work with this rabbit HF model.[11] However, some studies suggested that acute CaMKII inhibition could reduce I_{K1} in myocytes.[19, 41] We cannot readily explain the differences, but one of these studies was in rabbit, using less physiological conditions, square voltage clamp pulses, and short-term cell culture to overexpress CaMKIIδ.[19] Moreover, these studies showed that CaMKIIδ overexpression in either transgenic mice or in 24 hr in rabbit myocytes induced downregulation of I_{K1} and $K_{ir}2.1$. Since CaMKII is upregulated at the protein and activity level in HF, CaMKII-induced downregulation may explain the dominant I_{K1} downregulation that we saw in HF. Conceivably, our preincubation with the CaMKII inhibitor AIP increased channel expression, to coincidentally offset an acute inhibitory effect on channel function.

Surprisingly, both I_{Kr} and I_{Ks} densities were increased during the AP in HF, under physiological AP conditions (Fig. 3–4). However, in both cases this enhancement was abolished by strong $[Ca^{2+}]_i$ buffering, and for I_{Ks} by CaMKII inhibition. Ca^{2+}-sensitivity of delayed rectifier K^+ currents is well known, but details in the myocyte environment are still under debate.[42–46] For I_{Ks}, calmodulin (CaM) is an intrinsic subunit of the channel, and is known to mediate Ca^{2+}-dependent stimulation of I_{Ks} amplitude.[42–44] So, the $BAPTA_i$ effect to reduce I_{Ks} during the AP in HF is consistent with the myocyte Ca^{2+} transient boosting I_{Ks} during the AP. But in Control myocytes, $[Ca^{2+}]_i$ buffering had no effect on I_{Kr} or I_{Ks} under AP-clamp. The observation that CaMKII inhibition prevented the increased I_{Ks} in HF (but had no effect in Control) might provide a clue explaining this apparent dichotomy. That is, if CaMKII activity (which is elevated in HF),[20] promotes the intrinsic Ca^{2+} effect on I_{Ks} gating, AIP could suppress that Ca^{2+}-dependent I_{Ks} activation. The lower CaMKII activity in Control could limit that Ca^{2+}-dependent I_{Ks} activation, explaining the lack of $BAPTA_i$ or AIP on I_{Ks} in Control. In any case, basal I_{Ks} is small compared to I_{Kr} or I_{K1}, so its role in shaping the basal AP is moderate, but slightly stronger in HF.

I_{Kr} upregulation was Ca^{2+}-dependent, but CaMKII-independent. I_{Kr} is not known to be directly regulated by Ca^{2+} or CaM, but protein kinase C (PKC) has been reported to increase I_{Kr},[47] be increased in HF;[48, 49] and its Ca^{2+}-dependence makes this an intriguing possibility (although others found that PKC activation decreased I_{Kr} density[50]). Regardless of Ca^{2+}, I_{Kr} is higher early in the AP in HF vs. Control, suggesting potential changes in channel gating. Possible explanations might be HF-associated alterations in subunit composition or splice variants of the channel,[51] and chronic β-AR activation (which occurs in HF) positively shifts the HERG activation voltage, independent of actual PKA activity.[52] Further studies are needed to elucidate the underlying molecular mechanisms for I_{Kr} and I_{Ks} upregulation in HF and the exact involvement of Ca^{2+}, CaMKII and PKC in their regulation.

β-adrenergic induced changes in repolarizing K^+ currents in HF

β-AR stimulation is critical in the regulation of the heart in health and disease. Increased sympathetic activity is compensatory in early HF, but chronic β-AR activation also contributes to adverse remodeling in HF. On the other hand, cardiac contractile system and Ca^{2+} handling system are hyporesponsive to β-AR stimulation in HF.[11]

I_{Ks} is known to be increased by both PKA and Ca^{2+}/CaM in ventricular myocytes[44] and thus contributes to AP shortening upon β-AR stimulation (compensating for higher inward Ca^{2+} and Na^+/Ca^{2+} exchange currents).[27, 53] We found that the ISO-induced increase in I_{Ks} was suppressed in HF (both in physiological and $BAPTA_i$ conditions; Fig. 6D). Indeed, the ISO effect without $[Ca^{2+}]_i$ transients was smaller in HF, as was the increase by allowing $[Ca^{2+}]_i$ transients in HF. The EC_{50} ISO concentration for I_{Ks} (or I_{Kr}) activation was not altered in HF, but the maximal effect was less than half in HF vs. age-matched control (Fig. 7). This may be due to the reduced number of sarcolemmal β_1-AR in this HF model,[54] and lower local cAMP levels in HF[55] might explain the reduced ISO-response. Additionally, phosphatases and phosphosdiesterases are also remodeled in HF,[17] which may limit I_{Ks} target phosphorylation in HF. I_{Kr} was much less affected by β-AR stimulation than I_{Ks} in our study and in previous reports[27, 53] (~10 fold larger change in I_{Ks} than in I_{Kr} upon β-AR stimulation), but I_{Kr} changes are still debated. The β-adrenergic regulation of I_{Kr} may have species differences and involve both PKA and PKC.

I_{Kr}, I_{Ks} and I_{K1} reach their peak density sequentially during phase 3 of AP and their relative contributions to physiological repolarization and repolarization reserve differ, as demonstrated previously in control ventricular myocytes in detail.[27, 56, 57] In this study we demonstrated their detailed contribution to repolarization in a chronic pressure/volume overload-induced HF model (Fig. 8). Important to note, that inward currents, such as late Na^+ current[16] and Na^+/Ca^{2+} exchanger current,[22] are also increased in HF and β-AR further enhances inward Na^+/Ca^{2+} exchange and Ca^{2+} current. These increase the demand on the repolarization reserve during phase 3 of the AP to limit APD prolongation. Therefore, any change in the delicate balance between these depolarizing and repolarizing currents in HF could have significant impact on phase 3 repolarization velocity and thus on APD. Accordingly, the observed Ca^{2+}-dependent upregulation of I_{Kr} and I_{Ks} in HF may partly compensate for the loss of I_{K1} in HF and limits APD prolongation, especially at faster pacing rates when I_{Kr} may accumulate.[58] In line with our findings QT_c prolongation in HF

patients occurs preferentially at low but not at high heart rates.[15] However, as we have shown in Fig. 8, β-AR stimulation impairs the repolarization reserve capacity because of the hyporesponsive I_{Ks}.

These results also put heart rate reducing agents in HF therapy into a new perspective. The rationale of this strategy is to increase diastolic interval by which the myocardial oxygen supply/demand can be improved. Nevertheless, large clinical trials (BEATIFUL[59] and SHIFT[60] trials) found only a slight benefit of ivabradine in HF patients. Our results also suggest that β-AR blockers might have more benefit regarding K^+ currents and AP repolarization reserve, thus susceptibility for cardiac arrhythmias might be more reduced compared to that with heart-rate reducing agents. Another potential clinical implication is that drugs inhibiting delayed rectifier K^+ currents may cause even more pronounced QT_c prolongation in HF patients by limiting an already diminished repolarization reserve in HF, especially during β-AR stimulation.

Supplementary Material

Refer to Web version on PubMed Central for supplementary material.

Acknowledgments

We thank Logan R. J. Bailey, Johanna M. Borst, Maura Ferrero, Matthew L. Stein, Ian P. Palmer and Maximilien Bergman for their help in animal care and cell isolation.

Sources of Funding: This work was supported by grants from the National Institute of Health R01-HL30077 and P01-080101 (DMB), R01HL90880 (LTI and YCI), R01HL123526 (YCI) and the American Heart Association 14GRNT20510041 (YCI), 15GRNT25860028 (SMP).

References

1. Tomaselli GF, Beuckelmann DJ, Calkins HG, Berger RD, Kessler PD, Lawrence JH, Kass D, Feldman AM, Marban E. Sudden cardiac death in heart failure. The role of abnormal repolarization. Circulation. 1994; 90:2534–2539. [PubMed: 7955213]
2. Watanabe E, Arakawa T, Uchiyama T, Tong M, Yasui K, Takeuchi H, Terasawa T, Kodama I, Hishida H. Prognostic significance of circadian variability of RR and QT intervals and QT dynamicity in patients with chronic heart failure. Heart Rhythm. 2007; 4:999–1005. [PubMed: 17675071]
3. Arsenos P, Gatzoulis KA, Dilaveris P, Gialernios T, Sideris S, Lazaros G, Archontakis S, Tsiachris D, Kartsagoulis E, Stefanadis C. The rate-corrected QT interval calculated from 24-hour holter recordings may serve as a significant arrhythmia risk stratifier in heart failure patients. Int J Cardiol. 2011; 147:321–323. [PubMed: 21239068]
4. Algra A, Tijssen JGP, Roelandt JRTC, Pool J, Lubsen J. QTc prolongation measured by standard 12-lead electrocardiography is an independent risk factor for sudden-death due to cardiac-arrest. Circulation. 1991; 83:1888–1894. [PubMed: 2040041]
5. Piccirillo G, Magri D, Matera S, Magnanti M, Torrini A, Pasquazzi E, Schifano E, Velitti S, Marigliano V, Quaglione R, Barilla F. QT variability strongly predicts sudden cardiac death in asymptomatic subjects with mild or moderate left ventricular systolic dysfunction: A prospective study. Eur Heart J. 2007; 28:1344–1350. [PubMed: 17101636]
6. Vrtovec B, Knezevic I, Poglajen G, Sebestjen M, Okrajsek R, Haddad F. Relation of b-type natriuretic peptide level in heart failure to sudden cardiac death in patients with and without QT interval prolongation. Am J Cardiol. 2013; 111:886–890. [PubMed: 23273526]

7. Beuckelmann DJ, Nabauer M, Erdmann E. Alterations of K^+ currents in isolated human ventricular myocytes from patients with terminal heart failure. Circ Res. 1993; 73:379–385. [PubMed: 8330380]
8. Li GR, Lau CP, Leung TK, Nattel S. Ionic current abnormalities associated with prolonged action potentials in cardiomyocytes from diseased human right ventricles. Heart Rhythm. 2004; 1:460–468. [PubMed: 15851200]
9. Kaab S, Nuss HB, Chiamvimonvat N, O'Rourke B, Pak PH, Kass DA, Marban E, Tomaselli GF. Ionic mechanism of action potential prolongation in ventricular myocytes from dogs with pacing-induced heart failure. Circ Res. 1996; 78:262–273. [PubMed: 8575070]
10. Tsuji Y, Zicha S, Qi XY, Kodama I, Nattel S. Potassium channel subunit remodeling in rabbits exposed to long-term bradycardia or tachycardia: Discrete arrhythmogenic consequences related to differential delayed-rectifier changes. Circulation. 2006; 113:345–355. [PubMed: 16432066]
11. Pogwizd SM, Schlotthauer K, Li L, Yuan W, Bers DM. Arrhythmogenesis and contractile dysfunction in heart failure: Roles of sodium-calcium exchange, inward rectifier potassium current, and residual beta-adrenergic responsiveness. Circ Res. 2001; 88:1159–1167. [PubMed: 11397782]
12. Rose J, Armoundas AA, Tian Y, DiSilvestre D, Burysek M, Halperin V, O'Rourke B, Kass DA, Marban E, Tomaselli GF. Molecular correlates of altered expression of potassium currents in failing rabbit myocardium. Am J Physiol Heart Circ Physiol. 2005; 288:H2077–2087. [PubMed: 15637125]
13. Li GR, Lau CP, Ducharme A, Tardif JC, Nattel S. Transmural action potential and ionic current remodeling in ventricles of failing canine hearts. Am J Physiol Heart Circ Physiol. 2002; 283:H1031–1041. [PubMed: 12181133]
14. Rozanski GJ, Xu Z, Whitney RT, Murakami H, Zucker IH. Electrophysiology of rabbit ventricular myocytes following sustained rapid ventricular pacing. J Mol Cell Cardiol. 1997; 29:721–732. [PubMed: 9140829]
15. Davey PP, Barlow C, Hart G. Prolongation of the QT interval in heart failure occurs at low but not at high heart rates. Clin Sci (Lond). 2000; 98:603–610. [PubMed: 10781393]
16. Valdivia CR, Chu WW, Pu J, Foell JD, Haworth RA, Wolff MR, Kamp TJ, Makielski JC. Increased late sodium current in myocytes from a canine heart failure model and from failing human heart. J Mol Cell Cardiol. 2005; 38:475–483. [PubMed: 15733907]
17. Ai X, Curran JW, Shannon TR, Bers DM, Pogwizd SM. Ca^{2+}/calmodulin-dependent protein kinase modulates cardiac ryanodine receptor phosphorylation and sarcoplasmic reticulum Ca^{2+} leak in heart failure. Circ Res. 2005; 97:1314–1322. [PubMed: 16269653]
18. Wagner S, Dybkova N, Rasenack EC, Jacobshagen C, Fabritz L, Kirchhof P, Maier SK, Zhang T, Hasenfuss G, Brown JH, Bers DM, Maier LS. Ca^{2+}/calmodulin-dependent protein kinase II regulates cardiac Na^+ channels. J Clin Invest. 2006; 116:3127–3138. [PubMed: 17124532]
19. Wagner S, Hacker E, Grandi E, Weber SL, Dybkova N, Sossalla S, Sowa T, Fabritz L, Kirchhof P, Bers DM, Maier LS. Ca/calmodulin kinase II differentially modulates potassium currents. Circ Arrhythm Electrophysiol. 2009; 2:285–294. [PubMed: 19808479]
20. Anderson ME, Brown JH, Bers DM. CaMKII in myocardial hypertrophy and heart failure. J Mol Cell Cardiol. 2011; 51:468–473. [PubMed: 21276796]
21. Hoeker GS, Hanafy MA, Oster RA, Bers DM, Pogwizd SM. Reduced arrhythmia inducibility with calcium/calmodulin-dependent protein kinase II inhibition in heart failure rabbits. J Cardiovasc Pharmacol. 2016; 67:260–265. [PubMed: 26650851]
22. Pogwizd SM, Qi M, Yuan WL, Samarel AM, Bers DM. Upregulation of Na^+/Ca^{2+} exchanger expression and function in an arrhythmogenic rabbit model of heart failure. Circ Res. 1999; 85:1009–1019. [PubMed: 10571531]
23. Despa S, Islam MA, Weber CR, Pogwizd SM, Bers DM. Intracellular Na^+ concentration is elevated in heart failure but Na/K pump function is unchanged. Circulation. 2002; 105:2543–2548. [PubMed: 12034663]
24. Zima AV, Bovo E, Bers DM, Blatter LA. Ca^{2+} spark-dependent and -independent sarcoplasmic reticulum Ca^{2+} leak in normal and failing rabbit ventricular myocytes. J Physiol. 2010; 588:4743–4757. [PubMed: 20962003]

25. Uchinoumi H, Yang Y, Oda T, Li N, Alsina KM, Puglisi JL, Chen-Izu Y, Cornea RL, Wehrens XH, Bers DM. CaMKII-dependent phosphorylation of RyR2 promotes targetable pathological RyR2 conformational shift. J Mol Cell Cardiol. 2016; 98:62–72. [PubMed: 27318036]
26. Banyasz T, Horvath B, Jian Z, Izu LT, Chen-Izu Y. Sequential dissection of multiple ionic currents in single cardiac myocytes under action potential-clamp. J Mol Cell Cardiol. 2011; 50:578–581. [PubMed: 21215755]
27. Banyasz T, Jian Z, Horvath B, Khabbaz S, Izu LT, Chen-Izu Y. Beta-adrenergic stimulation reverses the I Kr-I Ks dominant pattern during cardiac action potential. Pflugers Arch. 2014; 466:2067–2076. [PubMed: 24535581]
28. Nichols CB, Chang CW, Ferrero M, Wood BM, Stein ML, Ferguson AJ, Ha D, Rigor RR, Bossuyt S, Bossuyt J. Beta-adrenergic signaling inhibits Gq-dependent protein kinase D activation by preventing protein kinase D translocation. Circ Res. 2014; 114:1398–1409. [PubMed: 24643961]
29. Banyasz T, Horvath B, Jian Z, Izu LT, Chen-Izu Y. Profile of L-type Ca^{2+} current and Na^{+}/Ca^{2+} exchange current during cardiac action potential in ventricular myocytes. Heart Rhythm. 2012; 9:134–142. [PubMed: 21884673]
30. Johnson DM, Heijman J, Bode EF, Greensmith DJ, van der Linde H, Abi-Gerges N, Eisner DA, Trafford AW, Volders PG. Diastolic spontaneous calcium release from the sarcoplasmic reticulum increases beat-to-beat variability of repolarization in canine ventricular myocytes after beta-adrenergic stimulation. Circ Res. 2013; 112:246–256. [PubMed: 23149594]
31. Szentandrassy N, Kistamas K, Hegyi B, Horvath B, Ruzsnavszky F, Vaczi K, Magyar J, Banyasz T, Varro A, Nanasi PP. Contribution of ion currents to beat-to-beat variability of action potential duration in canine ventricular myocytes. Pflugers Arch. 2015; 467:1431–1443. [PubMed: 25081243]
32. Bassani RA, Altamirano J, Puglisi JL, Bers DM. Action potential duration determines sarcoplasmic reticulum Ca^{2+} reloading in mammalian ventricular myocytes. J Physiol. 2004; 559:593–609. [PubMed: 15243136]
33. Shannon TR, Pogwizd SM, Bers DM. Elevated sarcoplasmic reticulum Ca^{2+} leak in intact ventricular myocytes from rabbits in heart failure. Circ Res. 2003; 93:592–594. [PubMed: 12946948]
34. Curran J, Brown KH, Santiago DJ, Pogwizd S, Bers DM, Shannon TR. Spontaneous Ca waves in ventricular myocytes from failing hearts depend on Ca^{2+}-calmodulin-dependent protein kinase II. J Mol Cell Cardiol. 2010; 49:25–32. [PubMed: 20353795]
35. Lengyel C, Iost N, Virag L, Varro A, Lathrop DA, Papp JG. Pharmacological block of the slow component of the outward delayed rectifier current (I_{Ks}) fails to lengthen rabbit ventricular muscle QT_c and action potential duration. Br J Pharmacol. 2001; 132:101–110. [PubMed: 11156566]
36. Zaza A, Rocchetti M, Brioschi A, Cantadori A, Ferroni A. Dynamic Ca^{2+}-induced inward rectification of K^{+} current during the ventricular action potential. Circ Res. 1998; 82:947–956. [PubMed: 9598592]
37. Straus SM, Kors JA, De Bruin ML, van der Hooft CS, Hofman A, Heeringa J, Deckers JW, Kingma JH, Sturkenboom MC, Stricker BH, Witteman JC. Prolonged QTc interval and risk of sudden cardiac death in a population of older adults. J Am Coll Cardiol. 2006; 47:362–367. [PubMed: 16412861]
38. Barr CS, Naas A, Freeman M, Lang CC, Struthers AD. QT dispersion and sudden unexpected death in chronic heart failure. Lancet. 1994; 343:327–329. [PubMed: 7905146]
39. Grimm M, Ling H, Willeford A, Pereira L, Gray CB, Erickson JR, Sarma S, Respress JL, Wehrens XH, Bers DM, Brown JH. CaMKIIdelta mediates beta-adrenergic effects on RyR2 phosphorylation and SR Ca^{2+} leak and the pathophysiological response to chronic beta-adrenergic stimulation. J Mol Cell Cardiol. 2015; 85:282–291. [PubMed: 26080362]
40. Kaab S, Dixon J, Duc J, Ashen D, Nabauer M, Beuckelmann DJ, Steinbeck G, McKinnon D, Tomaselli GF. Molecular basis of transient outward potassium current downregulation in human heart failure - a decrease in Kv4.3 mRNA correlates with a reduction in current density. Circulation. 1998; 98:1383–1393. [PubMed: 9760292]

41. Nagy N, Acsai K, Kormos A, Sebok Z, Farkas AS, Jost N, Nanasi PP, Papp JG, Varro A, Toth A. $[Ca^{2+}]_i$-induced augmentation of the inward rectifier potassium current (I_{K1}) in canine and human ventricular myocardium. Pflugers Arch. 2013; 465:1621–1635. [PubMed: 23807312]
42. Tohse N. Calcium-sensitive delayed rectifier potassium current in guinea pig ventricular cells. Am J Physiol. 1990; 258:H1200–1207. [PubMed: 2331008]
43. Xie Y, Ding WG, Matsuura H. Ca^{2+}/calmodulin potentiates I_{Ks} in sinoatrial node cells by activating Ca^{2+}/calmodulin-dependent protein kinase ii. Pflugers Arch. 2015; 467:241–251. [PubMed: 24737247]
44. Bartos DC, Morotti S, Ginsburg KS, Grandi E, Bers DM. Quantitative analysis of the Ca^{2+}-dependent regulation of delayed rectifier K^+ current I_{Ks} in rabbit ventricular myocytes. J Physiol. 2017; 595:2253–2268. [PubMed: 28008618]
45. Nitta J, Furukawa T, Marumo F, Sawanobori T, Hiraoka M. Subcellular mechanism for Ca^{2+}-dependent enhancement of delayed rectifier K^+ current in isolated membrane patches of guinea-pig ventricular myocytes. Circ Res. 1994; 74:96–104. [PubMed: 8261599]
46. Ghosh S, Nunziato DA, Pitt GS. KCNQ1 assembly and function is blocked by long-QT syndrome mutations that disrupt interaction with calmodulin. Circ Res. 2006; 98:1048–1054. [PubMed: 16556866]
47. Heath BM, Terrar DA. Protein kinase c enhances the rapidly activating delayed rectifier potassium current, I_{Kr}, through a reduction in c-type inactivation in guinea-pig ventricular myocytes. J Physiol. 2000; 522:391–402. [PubMed: 10713964]
48. Bowling N, Walsh RA, Song G, Estridge T, Sandusky GE, Fouts RL, Mintze K, Pickard T, Roden R, Bristow MR, Sabbah HN, Mizrahi JL, Gromo G, King GL, Vlahos CJ. Increased protein kinase C activity and expression of Ca^{2+}-sensitive isoforms in the failing human heart. Circulation. 1999; 99:384–391. [PubMed: 9918525]
49. Braz JC, Gregory K, Pathak A, Zhao W, Sahin B, Klevitsky R, Kimball TF, Lorenz JN, Nairn AC, Liggett SB, Bodi I, Wang S, Schwartz A, Lakatta EG, DePaoli-Roach AA, Robbins J, Hewett TE, Bibb JA, Westfall MV, Kranias EG, Molkentin JD. PKC-alpha regulates cardiac contractility and propensity toward heart failure. Nat Med. 2004; 10:248–254. [PubMed: 14966518]
50. Cockerill SL, Tobin AB, Torrecilla I, Willars GB, Standen NB, Mitcheson JS. Modulation of hERG potassium currents in HEK-293 cells by protein kinase C. Evidence for direct phosphorylation of pore forming subunits. J Physiol. 2007; 581:479–493. [PubMed: 17363390]
51. Holzem KM, Gomez JF, Glukhov AV, Madden EJ, Koppel AC, Ewald GA, Trenor B, Efimov IR. Reduced response to IKr blockade and altered hERG1a/1b stoichiometry in human heart failure. J Mol Cell Cardiol. 2016; 96:82–92. [PubMed: 26093152]
52. Shu L, Zhang W, Su G, Zhang J, Liu C, Xu J. Modulation of hERG K^+ channels by chronic exposure to activators and inhibitors of PKA and PKC: Actions independent of PKA and PKC phosphorylation. Cell Physiol Biochem. 2013; 32:1830–1844. [PubMed: 24356123]
53. Szentandrassy N, Farkas V, Barandi L, Hegyi B, Ruzsnavszky F, Horvath B, Banyasz T, Magyar J, Marton I, Nanasi PP. Role of action potential configuration and the contribution of Ca^{2+} and K^+ currents to isoprenaline-induced changes in canine ventricular cells. Br J Pharmacol. 2012; 167:599–611. [PubMed: 22563726]
54. Desantiago J, Ai X, Islam M, Acuna G, Ziolo MT, Bers DM, Pogwizd SM. Arrhythmogenic effects of beta2-adrenergic stimulation in the failing heart are attributable to enhanced sarcoplasmic reticulum ca load. Circ Res. 2008; 102:1389–1397. [PubMed: 18467626]
55. Barbagallo F, Xu B, Reddy GR, West T, Wang Q, Fu Q, Li M, Shi Q, Ginsburg KS, Ferrier W, Isidori AM, Naro F, Patel HH, Bossuyt J, Bers D, Xiang YK. Genetically encoded biosensors reveal PKA hyperphosphorylation on the myofilaments in rabbit heart failure. Circ Res. 2016; 119:931–943. [PubMed: 27576469]
56. Banyasz T, Magyar J, Szentandrassy N, Horvath B, Birinyi P, Szentmiklosi J, Nanasi PP. Action potential clamp fingerprints of K^+ currents in canine cardiomyocytes: Their role in ventricular repolarization. Acta Physiol (Oxf). 2007; 190:189–198. [PubMed: 17394574]
57. Jost N, Virag L, Bitay M, Takacs J, Lengyel C, Biliczki P, Nagy Z, Bogats G, Lathrop DA, Papp JG, Varro A. Restricting excessive cardiac action potential and QT prolongation: A vital role for I_{Ks} in human ventricular muscle. Circulation. 2005; 112:1392–1399. [PubMed: 16129791]

58. Jurkiewicz NK, Sanguinetti MC. Rate-dependent prolongation of cardiac action potentials by a methanesulfonanilide class III antiarrhythmic agent. Specific block of rapidly activating delayed rectifier K^+ current by dofetilide. Circ Res. 1993; 72:75–83. [PubMed: 8417848]

59. Fox K, Ford I, Steg PG, Tendera M, Ferrari R. Investigators B. Ivabradine for patients with stable coronary artery disease and left-ventricular systolic dysfunction (BEAUTIFUL): A randomised, double-blind, placebo-controlled trial. Lancet. 2008; 372:807–816. [PubMed: 18757088]

60. Swedberg K, Komajda M, Bohm M, Borer JS, Ford I, Dubost-Brama A, Lerebours G, Tavazzi L. Investigators S. Ivabradine and outcomes in chronic heart failure (SHIFT): A randomised placebo-controlled study. Lancet. 2010; 376:875–885. [PubMed: 20801500]

What is Known?

- Ion channel remodeling occurs in heart failure resulting in prolongation of the cardiac action potential (and QT interval on the ECG), predominantly at low heart rates.
- Prolonged action potential is associated with increased risk of cardiac arrhythmias.

What the Study Adds?

- Calcium/CaMKII-dependent increases of delayed rectifier K^+ currents (I_{Kr}, I_{Ks}) compensate for the decrease of inward rectifier K^+ current (I_{K1}) in heart failure (0t higher heart rates).
- Reduced beta-adrenergic responsiveness of I_{Ks} severely limits repolarization reserve in heart failure during sympathetic stimulation, further increasing arrhythmia risk.

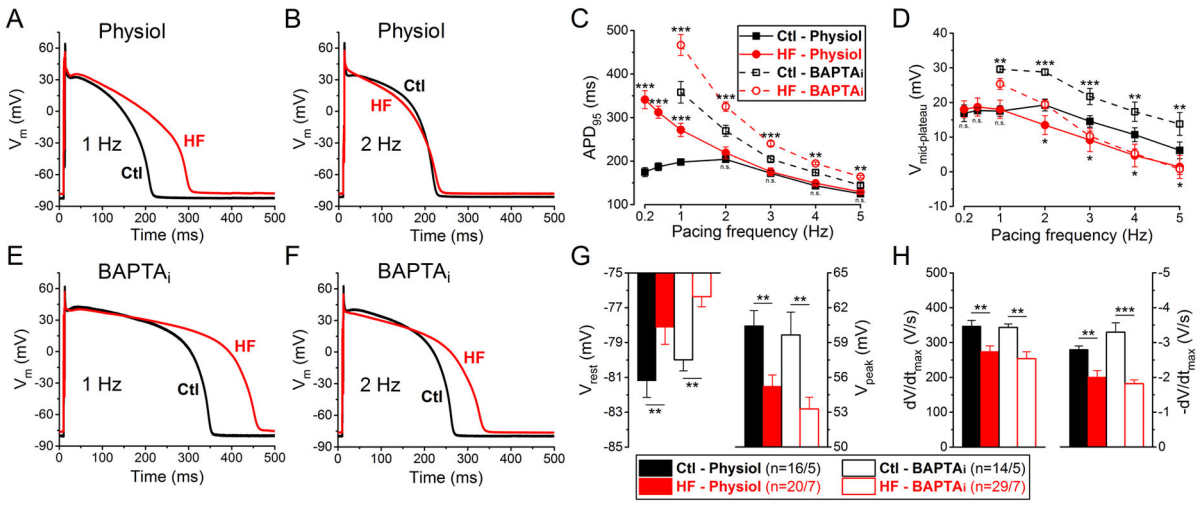

Figure 1. Frequency- and Ca^{2+}-dependent changes of AP parameters in HF

(**A–B**) Representative action potentials (APs) recorded at 1 Hz and 2 Hz pacing in heart failure (HF) and healthy age-matched control cells with physiological solutions (Physiol). (**C–D**) Frequency dependence of AP duration measured at 95% of repolarization (APD_{95}) and mid-plateau potential ($V_{mid\text{-}plateau}$). (**E–F**) Representative APs when cytosolic Ca^{2+} was buffered to nominally zero using 10 mM BAPTA in pipette solution ($BAPTA_i$) at 1 Hz and 2 Hz pacing. (**G**) Resting membrane potential (V_{rest}) is less negative in HF in line with decreased AP peak (V_{peak}) at 1 Hz. (**H**) Both maximal rate of rise (dV/dt_{max}) and maximal rate of phase 3 repolarization ($-dV/dt_{max}$) are significantly decreased in HF at 1 Hz. Columns and bars represent mean±SEM. *n* refers to cells/animals measured in each group. ANOVA with Bonferroni posttest, Ctl vs. HF, *p<0.05, **p<0.01, ***p<0.001.

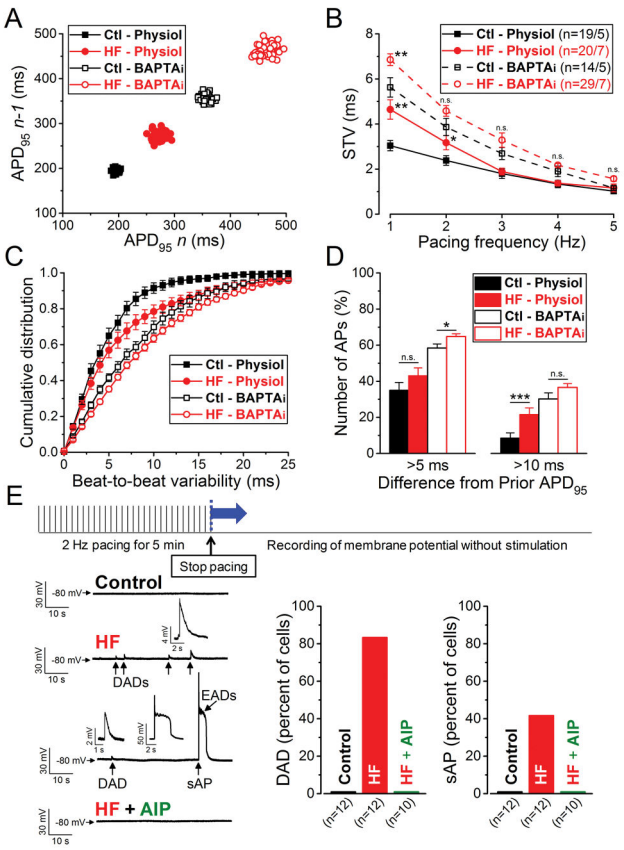

Figure 2. Increased temporal variability of APD and arrhythmogenesis in HF

(**A**) Representative Poincare plots of 50 consecutive APD_{95} values at 1 Hz steady-state pacing in 4 individual myocytes from HF and age-matched control animals recorded with either preserved or buffered $[Ca^{2+}]_i$. (**B**) Frequency-dependent short-term variability of APD_{95} (STV). (**C**) Cumulative distribution curves of individual beat-to-beat variability values at 1 Hz pacing. (**D**) Percentage of total APs measured at 1 Hz pacing having beat-to-beat APD_{95} variability of >5 ms and >10 ms in consecutive beats. Columns and bars represent mean±SEM. *n* refers to cells/animals measured in each group. ANOVA with Bonferroni posttest, *p<0.05, **p<0.01, ***p<0.001. (**E**) Arrhythmogenic diastolic activities were tested using the pacing protocol shown above. (Left) Representative records in control, HF and AIP (CaMKII inhibitor, 1 μM) treated HF cells are shown below. HF cells frequently showed delayed afterdepolarizations (DADs, enlarged in insets) and spontaneous AP (sAP, enlarged in inset). Early afterdepolarizations (EADs, enlarged in inset) were also superimposed on the sAP repolarization. (Right) Percentage of cells having DAD and sAP. 10/12 cells and 5/12 cells showed DADs and sAP in HF, respectively, whereas no DAD, sAP or EAD was observed in control and following AIP treatment in HF.

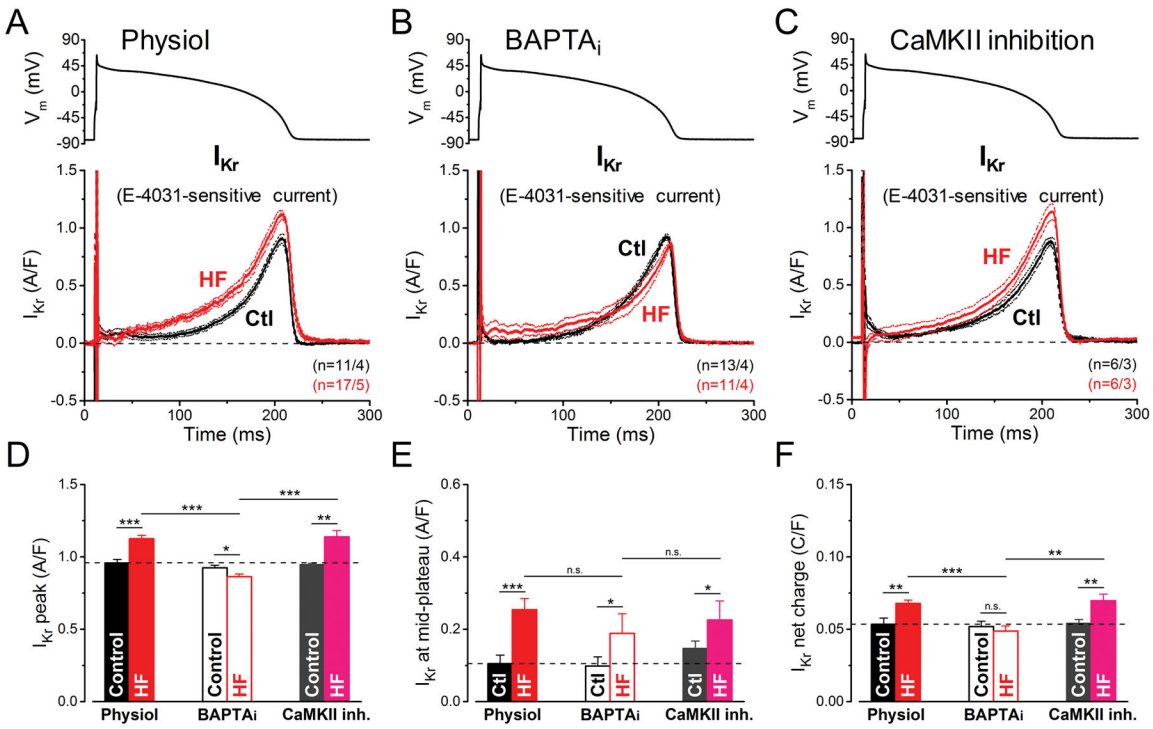

Figure 3. Ca^{2+}-dependent upregulation of I_{Kr} in HF under AP-clamp

The rapid component of delayed rectifier K^+ current (I_{Kr}) was measured as E-4031 (1 μM)-sensitive current in HF and age-matched control cells. AP-clamp using a prerecorded typical AP (shown above) was applied at 2 Hz. (**A**) I_{Kr} traces (mean±SEM) recorded under preserved $[Ca^{2+}]_i$ cycling (Physiol). I_{Kr} is not only increased in HF cells having $[Ca^{2+}]_i$ transients, but it activates earlier during the AP. (**B**) I_{Kr} traces (mean±SEM) recorded under buffered $[Ca^{2+}]_i$ using 10 mM BAPTA in the pipette ($BAPTA_i$). Buffering $[Ca^{2+}]_i$ significantly reduced I_{Kr} density in HF below the control level, but it had no effect in control. (**C**) I_{Kr} traces (mean±SEM) recorded in cells pretreated with the specific CaMKII inhibitor peptide AIP (1 μM). AIP had no effect on I_{Kr} both in control and in HF. (**D**) Peak I_{Kr} density is significantly upregulated in HF under AP by a Ca^{2+}-dependent, but CaMKII-independent pathway. (**E**) I_{Kr} density measured at the mid-plateau increased in HF indicating earlier I_{Kr} accumulation during AP, which occurred independent of $[Ca^{2+}]_i$ level and CaMKII activity. (**F**) Net charges carried by I_{Kr} in HF and age-matched control. Columns and bars represent mean±SEM. *n* refers to cells/animals measured in each group. ANOVA with Bonferroni posttest, *p<0.05, **p<0.01, ***p<0.001.

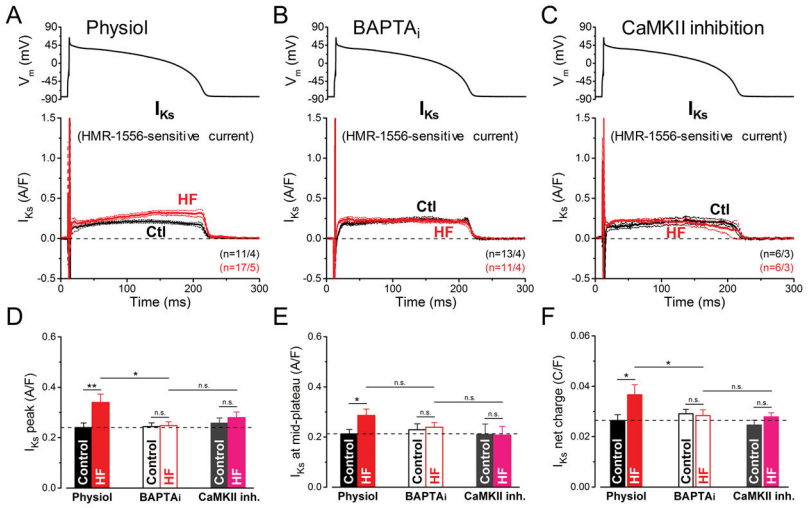

Figure 4. Ca^{2+}/CaMKII-dependent upregulation of I_{Ks} in HF under AP-clamp

The slow component of delayed rectifier K^+ current (I_{Ks}) was measured as HMR-1556 (1 μM)-sensitive current in HF and age-matched control cells. AP-clamp using a prerecorded typical AP (shown above) was applied at 2 Hz. (**A**) I_{Ks} traces (mean±SEM) recorded under preserved $[Ca^{2+}]_i$ cycling (Physiol). Basal I_{Ks} is a tiny current under AP, yet it is significantly upregulated in HF cells having $[Ca^{2+}]_i$ transients. (**B**) I_{Ks} traces (mean±SEM) recorded under buffered $[Ca^{2+}]_i$ using 10 mM BAPTA in the pipette ($BAPTA_i$). Buffering $[Ca^{2+}]_i$ reduced I_{Ks} in HF back to its control level. (**C**) I_{Ks} traces (mean±SEM) recorded in cells pretreated with the specific CaMKII inhibitor peptide AIP (1 μM). AIP abolished the I_{Ks} upregulation in HF. (**D**) Peak I_{Ks} density is significantly upregulated in HF under AP by a Ca^{2+}/CaMKII-dependent pathway. (**E**) I_{Ks} density measured at the mid-plateau of the AP. (**F**) Net charges carried by I_{Ks} in HF and age-matched control. Columns and bars represent mean±SEM. *n* refers to cells/animals measured in each group. ANOVA with Bonferroni posttest, *p<0.05, **p<0.01.

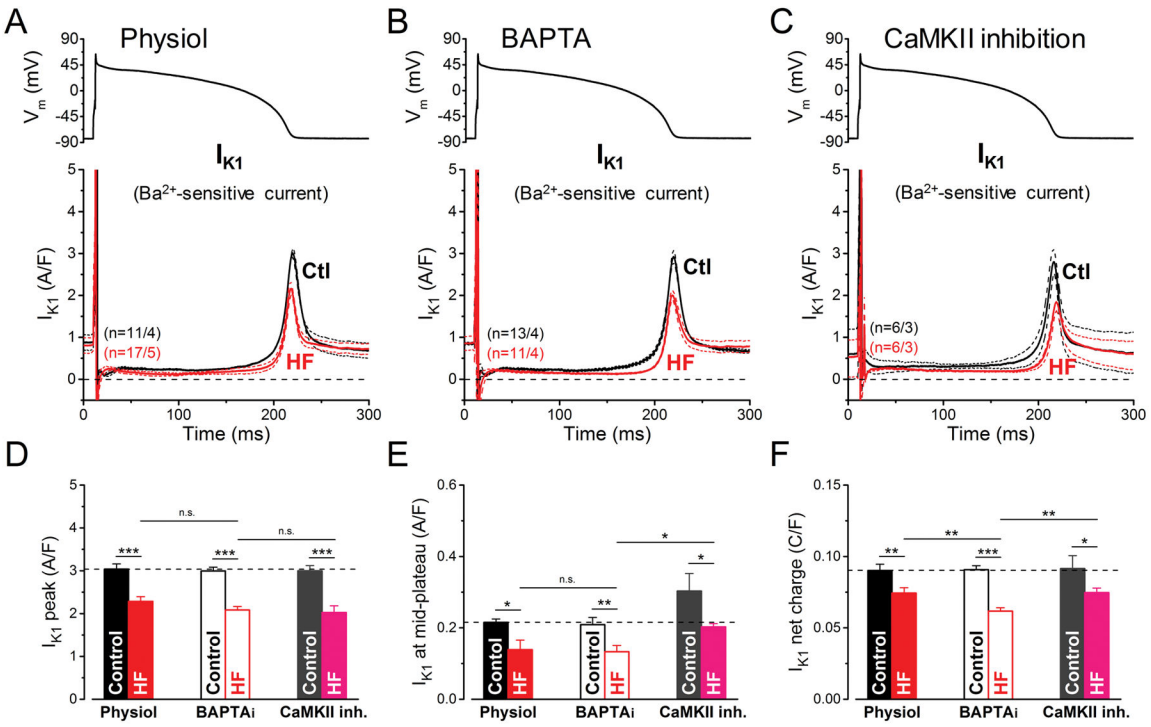

Figure 5. Reduction of I_{K1} in HF under AP-clamp

The inward rectifier K^+ current (I_{K1}) was measured as Ba^{2+} (100 μM)-sensitive current in HF and age-matched control cells. AP-clamp using a prerecorded typical AP (shown above) was applied at 2 Hz. (**A–C**) I_{K1} traces (mean±SEM) recorded under preserved $[Ca^{2+}]_i$ cycling (Physiol), $[Ca^{2+}]_i$ buffering ($BAPTA_i$) and CaMKII inhibition using AIP. I_{K1} was significantly reduced in HF in all these conditions. (**D–F**) Statistics for peak I_{K1} density shows that the reduction is not influenced by $[Ca^{2+}]_i$ buffering or acute CaMKII inhibition. (**E**) I_{K1} density measured at the mid-plateau of the AP was also reduced. (**F**) Net charges carried by I_{K1} was further reduced in HF when measured with $[Ca^{2+}]_i$ buffering. Columns and bars represent mean±SEM. *n* refers to cells/animals measured in each group. ANOVA with Bonferroni posttest, *p<0.05, **p<0.01, ***p<0.001.

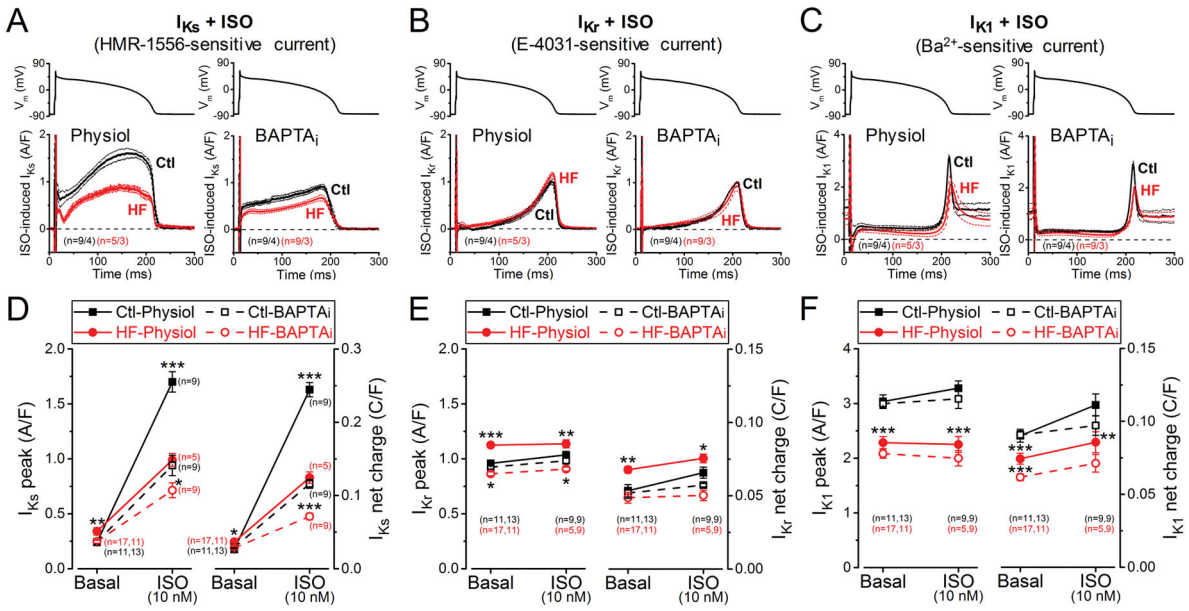

Figure 6. Altered response of K^+ currents to β-AR stimulation in HF

I_{Ks}, I_{Kr} and I_{K1} currents were recorded following 2 min pretreatment with beta-adrenergic receptor agonist isoproterenol (ISO, 10 nM). (**A**) I_{Ks} traces (mean±SEM) under canonical AP-clamp at 2 Hz measured with preserved $[Ca^{2+}]_i$ cycling (Physiol) and $[Ca^{2+}]_i$ buffering using 10 mM BAPTA in the pipette ($BAPTA_i$). (**B**) I_{Kr} traces (mean±SEM) under AP-clamp following ISO pretreatment in HF and age-matched control cells. (**C**) I_{K1} traces (mean ±SEM) under AP-clamp following ISO pretreatment in physiological solutions and in $BAPTA_i$. (**D**) Robust upregulation of I_{Ks} peak and net charge induced by ISO, which is reduced in $BAPTA_i$ indicating a Ca^{2+}-dependent pathway in mediating the response of β-AR stimulation on I_{Ks} besides the classical PKA-dependent phosphorylation. HF cells showed significantly reduced I_{Ks} accumulation upon ISO application both with and without $[Ca^{2+}]_i$ buffering. (**E**) I_{Kr} is slightly modulated by ISO both in control and HF. (**F**) I_{K1} peak density is not influenced by ISO, but I_{K1} net charge is slightly increased in HF due to altered rectification. Symbols and bars represent mean±SEM. *n* refers to cells measured in each group, and the cells in each group came from three to five individual animals. ANOVA with Bonferroni posttest, *p<0.05, **p<0.01, ***p<0.001.

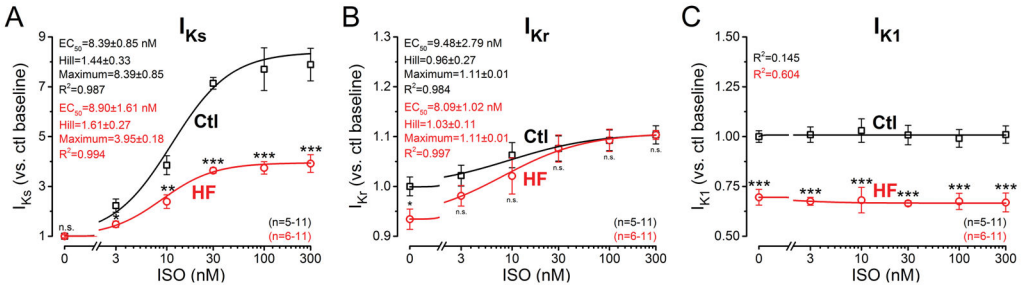

Figure 7. β-AR responsiveness of K^+ currents in HF

Dose-response effect of isoproterenol (ISO) on I_{Ks}, I_{Kr} and I_{K1} peak densities under AP-clamp at 2 Hz. Pipette solution contained 10 mM BAPTA. (**A**) I_{Ks} measured as HMR-sensitive current showed a robust accumulation following ISO application. I_{KS} sensitivity (EC_{50}) to ISO was unchanged in HF, whereas the response was significantly reduced in HF. (**B**) I_{Kr} was minimally affected by ISO treatment; however, neither the ISO-sensitivity nor the magnitude of the response were altered in HF. (**C**) I_{K1} peak density did not change following ISO application under buffered $[Ca^{2+}]_i$ conditions and I_{K1} was uniformly decreased in HF. EC_{50} values, Hill coefficients and maximum responses were determined by fitting data to the Hill equation, indicated by solid lines. Symbols and bars represent mean ±SEM. *n* refers to the number of cells measured in each group, and the cells in each group came from three to five individual animals. ANOVA with Bonferroni posttest, *p<0.05, **p<0.01, ***p<0.001.

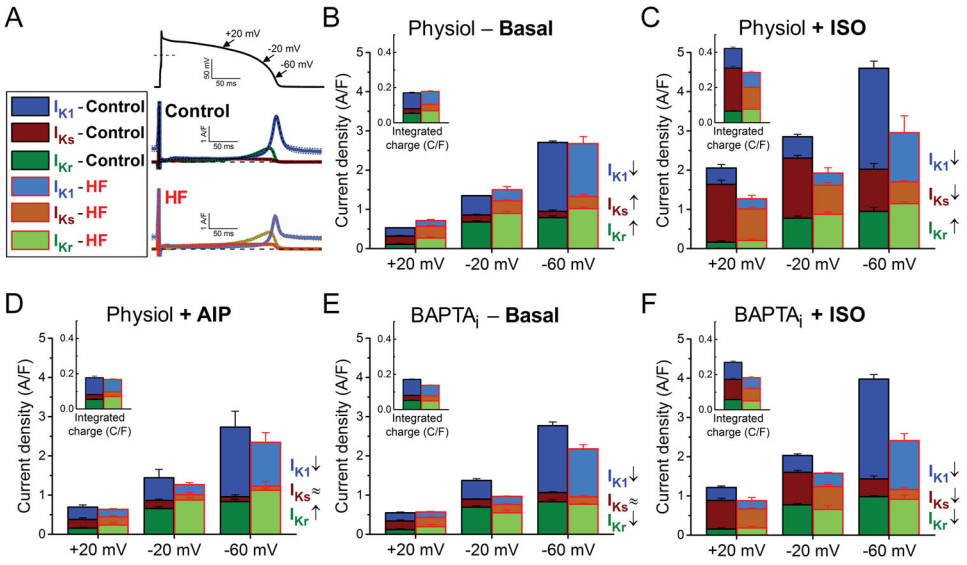

Figure 8. Relative contribution of each K^+ current to net repolarizing K^+ current in HF

Relative contributions and magnitudes of the major repolarizing K^+ currents (I_{Kr}, I_{Ks}, I_{K1}) during AP are compared in different phases of the repolarization process in HF to those in age-matched control. (**A**) I_{Kr}, I_{Ks} and I_{K1} traces in control and HF measured under AP-clamp at 2 Hz without using any Ca^{2+} buffer or β-AR agonist. Mean traces and SEM are shown. (**B**) When $[Ca^{2+}]_i$ cycling is preserved, upregulation of I_{Kr} and I_{Ks} compensates the decrease of I_{K1} in HF during phase 3 of AP. (**C**) Stimulation of β-ARs using isoproterenol (ISO, 10 nM) significantly upregulates I_{Ks}, thus ISO reverses I_{Kr}/I_{Ks} dominant pattern of repolarization during phase 3 of AP. However, HF cells are hyporesponsive to ISO-induced stimulation (i.e. I_{Ks} increases in a smaller extent than in control) thus the net repolarizing current is largely reduced in HF compared to control. Reversal in I_{Kr}/I_{Ks} dominance in repolarization following ISO treatment also fail to happen in HF. (**D**) CaMKII inhibition using the specific inhibitory peptide AIP abolishes the increase in I_{Ks}, whereas it does not affect I_{Kr} and I_{K1}. (**E**) When $[Ca^{2+}]_i$ is buffered ($BAPTA_i$), the reduction in I_{K1} without the upregulation of I_{Kr} and I_{Ks} results in a significant decrease in the net repolarizing current in HF. (**F**) Under β-adrenergic stimulation in $BAPTA_i$, HF cells show decrease in all three K^+ currents compared to control. The contributions of these K^+ currents to total net charge are shown in the insets. Columns and bars represent mean±SEM. Statistics and *n* numbers are shown in Figs. 3–6.

Table 1

Morphometric data of HF and age-matched control rabbits

Heart failure was induced in 10 rabbits and progression was assesed periodically by echocardiography. Data of HF rabbits at the time when cardiac myocytes were isolated are compared to 5 age-matched healthy control rabbits.

	Age-matched control	HF
Age (years)	2.40±0.17	2.46±0.35$^{n.s.}$
Body weight (kg)	3.99±0.14	3.98±0.13$^{n.s}$
Heart weight (g)	10.46±0.59	21.86±2.54***
HW/BW (g/kg)	2.63±0.15	5.52±0.71**
Lung weight (g)	13.86±0.25	18.94±1.16**
LW/BW (g/kg)	3.49±0.12	4.95±0.21**
LVESD (cm)	1.08±0.07	1.63±0.11***
LVEDD (cm)	1.71±0.07	2.29±0.09***
FS (%)	36.70±2.02	28.39±1.13*

All data represent mean±SEM. Unpaired, two-tailed Student's *t* test;

* $p<0.05$,

** $p<0.01$,

*** $p<0.001$.

(HW/BW, heart weight–to–body weight ratio; LW/BW, lung weight–to–body weight ratio LVESD, left ventricular end-systolic diameter; LVEDD, left ventricular end-diastolic diameter; FS, fractional shortening calculated as FS=(LVEDD-LVESD)/LVEDD*100)